# Time reversal symmetry breaking in cuprates induced by the spiral spin order.

M.Ya.Ovchinnikova

*Joint Institute of Chemical Physics of RAS, Kosygin str.,4, 117334, Moscow, Russia*

We propose a new interpretation of the spontaneous time reversal symmetry breaking (TRSB) observed recently in a pseudogap state of cuprates (Kaminsky et al.). It is shown that the TRSB dichroism in ARPES signal may be connected with the local spin spiral structures in system. It may be caused by a spin-orbit interaction and by spin polarization of electrons at various sections of Fermi surface in spiral state. Angular dependence of dichroism signal is studied in schematic KKR approximation. Tests are proposed to check an existence of the local spiral spin structure and to distinguish it from the TRSB state with micro-currents constructed by Varma.

Pacs: 71.10.Fd, 74.20.Rp, 74.20.-z

The nature of a pseudogap (PS) state of high-$T_c$ cuprates in underdoped (UD) region remains the intriguing problem [1,2]. Recently, using the angular-resolved photoemission (ARPES) with circularly polarized light (CPL), Kaminsky et al. [3] reveal new property of the pseudogap state of UD $Bi_2Sr_2CaCu_2O_{8-\delta}$ (BSCCO). It was shown that this state displays a spontaneous time-reversal symmetry breaking (TRSB). Earlier Varma [4] had predicted the possibility of TRSB in cuprates. They proposed the fascinate ground state with circular microcurrents inside the plaquettes of $CuO_2$ plane with definite alignment of orbital angular momenta associated with these micro-currents. Namely, the up-directed orbital momenta arrange along one diagonal and the down-directed orbital momenta arrange along other diagonal. The proposed in [4,5] alignment of orbital angular momenta is not connected with any spin alignment.

The aim of present paper is to discuss an alternative possibility for constructing the state with TRSB. Here we propose a state in which the TRSB is due to a spiral spin structure. The arguments in favor of such hypothesis are following. The electric field of CPL really interacts only with the orbital motion. Therefore the TRSB dichroism implies a definite orientation of orbital angular momenta $< L_n > \neq 0$. Such momenta, centered on the atoms, may be induced by aligned spin momenta $< S_n > \neq 0$ through the spin-orbit interaction. This means that in ARPES one could observe a TRSB dichroism $D$ if the photoemission setup can selectively measure the ejected electrons with definite spin projection $\sigma = \uparrow$ or $\downarrow$. Then a sign of the TRSB dichroism would depend on a sign of $\sigma$. Since usually the ARPES is non-selective with respect to the final spin projection of an ejected electron, the summary TRSB dichroism is expected to be zero if a mean spin polarization of initial states is zero. But for the spiral spin structure the occupancy $n_{k\sigma}$ of initial one-electron band state $\{k\sigma\}$ with definite $k$ depends on $\sigma$. Such spin polarization of initial $k$-state may induce the non-zero TRSB effects in ARPES signal. So we calculate a dichroism which might manifest in ARPES in case of the spiral spin configuration of cuprates.

The scheme of experiment [3] is given in Fig. 1. The right (left) polarized light with a propagation vector $\mathbf{q}_\gamma$ impacts the crystal surface determined by a normal vector $\mathbf{n}$. The $xz$ plane is one of the mirror planes of crystal with x-axis along the $CuO$ bonds or along a diagonal direction. The ejected electron has a final momentum $\mathbf{k}_f$. The ARPES intensity $I \sim |M_{if}|^2 \delta(E_i - E_f - \hbar\omega)$ is determined by a matrix element of interaction $O = (e/2m_e c)(\mathbf{Ap} + \mathbf{pA})$ with field

$$M = A_\alpha F_\alpha; \quad F_\alpha = < \psi_f | p_\alpha | \psi_i(k) > \tag{1}$$

between initial and final states. In dipole approximation it contains the vector potential $\mathbf{A}$ of the right ($\zeta_R = 1$) or left ($\zeta_L = -1$) CPL with complex amplitude

$$\mathbf{A_{R(L)}} = A_0[\mathbf{e}_x \cos\theta_\gamma + i\zeta_{R(L)}\mathbf{e}_y + \mathbf{e}_z \sin\theta_\gamma] \tag{2}$$

For given configuration of the setup vectors $\mathbf{n}$, $\mathbf{k}_f$, $\mathbf{q}_\gamma$ the ARPES dichroism signal $D$ is determined by a relative difference of intensities for both light polarizations:

$$D = (M_R - M_L)/(M_R + M_L) \quad (3)$$

We study the symmetry properties of ARPES matrix elements with respect to reflection in a mirror plane of a crystal, which is perpendicular to the surface in a typical photoemission experiment. Following [3], consider first a time reversal invariant initial state $\psi_i(k)$ and let $\mathbf{q}_\gamma$ and $\mathbf{n}$ lie in the mirror plane $m$ of crystal (here the $xz$ plane). Then, the dichroism signal $D$ is nonzero only if $\mathbf{k}_f$ does not lie in the mirror plane $m$ and D has an opposite signs for $k$ at different sides of mirror plane. Such dichroism is called a geometrical one. This large effect has been observed at any doping [3]. But in UD BSCCO the residual dichroism ($D \neq 0$) has been observed even for coplanar configuration of $\mathbf{n}$, $\mathbf{k}_f$, $\mathbf{q}_\gamma$, in which all three vectors lie in mirror plane $m$. Further we adopt a definitions $q_z$,$\mathbf{q}$ and $k_z$, $\mathbf{k}$ for the normal and 2D intra-layer components of the photon and final electron momenta $\mathbf{q}_\gamma$ and $\mathbf{k}_f$ correspondingly.

Consider first a large geometrical dichroism and then discuss a possible origin of the observed residual dichroism connected with TRSB of the ground state of UD cuprate. We suggest that the main contributions to matrix element give the space regions inside the atomic spheres. This is in accordance with a fact that the frequency dependencies of photoemission intensity roughly repeat the dependencies of the photoemission cross-sections coming from corresponding atomic components [6].

The formalism for evaluating the optical matrix element for general lattice within KKR scheme is given in [7]. Some corrections should be introduced to provide the common asymptotic $\sim e^{ik_f r}$ of the final wave function of the ejected electron outside the sample ($z > 0$). We restrict our consideration by the one-step model (see [8]) describing a coherent part of photoemission. Incorporation of rescattering and relaxation processes in frame of generalization to a three-step model are needed to describe the background in the energy distribution function of ejected electron. We believe that one-step model is sufficient to describe in qualitative manner the angular dependence of dichroism. For this aim we will use the most simplified form of the initial and final states in the process.

The starting point in calculating of $F_\alpha$ in (1) is the KKR wave function for a multicomponent lattice [7]. In Hartree-Fock representation the one-particle initial state $\psi_i$ with quasi-momentum $\mathbf{k}$ is a superposition of orbitals belonging to each center

$$\psi_i(r,k) = \frac{1}{\sqrt{N}} \sum_{n,\beta} B(n_z) e^{ikr} i^l C^i_{L\beta} \psi^i_{L\beta}(r - R_{n\beta}) \quad (4)$$

Here $\beta$ enumerates all atoms placed at $R_{n\beta}$ in unit cell $n = (n_x, n_y, n_z)$ and $L = l, m$ are the angular momentum quantum numbers of orbitals inside each atomic sphere $|r - R_{n\beta}| < a_{n\beta}$. For the upper valence anti-bonding band of $CuO_2$ plane the main orbitals $\psi^i_{L\beta}$ are the $d_{x^2-y^2}$ orbital of Cu and $p_x,\ p_y$ orbitals of two oxygens $O_x, O_y$. These orbitals constitute a basis set of the Emery model.

Thus the initial one-electron state is taken as superposition of the main real orbitals and in the second quantization representation it is

$$\psi_i(k,\sigma) = \sum_{n_z} B_i(n_z)[c_d d^\dagger_{k\sigma} + ic_x x^\dagger_{k\sigma} + ic_y y^\dagger_{k\sigma}] \quad (5)$$

The corresponding site operators $d^\dagger_{n\sigma}$, $x^\dagger_{n,\sigma}$, $y^\dagger_{n,\sigma}$ of Emery model refer to the real functions $d_{x^2-y^2}(r - R_{n,d})$, $p_\nu(r - R_{n,\nu})$ with $R_{n,\nu} = R_n + \mathbf{e}_\nu a/2$, $\nu = x, y$. The functions are considered to extend inside the corresponding atomic (muffin-tin) spheres. The real coefficients $c_d$, $c_x$, $c_y$ in (5) are obtained from solution of the Emery model. In Eq.(4,5) the term under the sum refer to a layer number $n_z$. The amplitudes $B(n_z)$ depending on distance of layer from the surface describe in phenomenological manner a coherent or incoherent interlayer transport along $z$ near the surface depending on the phase correlations between different layers. For standard bulk initial state $\psi_i$ used in [7] $B(n_z) \sim \exp(ik_z n_z)$.

A final state inside the sample is taken in similar KKR form with the same in-plane momentum $k$:

$$\psi_f = \frac{1}{\sqrt{N}} \sum_{n,\beta} B^f(n_z) e^{ikR_{n\beta}} i^l C_{L\beta} Y^*_L \psi_{L\beta}(r - R_{n\beta}) \quad (6)$$

Here each of functions $\psi_{L\beta}$ with angular momentum quantum numbers $L = (l, m)$ is determined inside atomic spheres around corresponding center $R_{n,\beta}$. Influence of surface at z=0 is described by introducing the factors $B^f(n_z)$, by phases $\delta_{l,\beta}$ of complex coefficients

$$C_{L\beta} = |C_{L\beta}| e^{\delta_{l\beta}}, \quad (7)$$

and by explicit angular spherical harmonics $Y_L = Y_{lm}(\hat{k}_f)$ depending on direction of final momentum $k_f$. The phases are specific for centers $\beta$ in unit cell and for angular momentum $l$. These phases arise from a matching of final state (6) inside the sample with the common plane wave $\sim e^{ik_f r}$ in empty space outside it. The phase modulation of contributions in (6) determines the geometrical dichroism of the photoemission.

The origin of spherical harmonics in Eq.(6) and of the phase modulation of coefficients (7) may be illustrated by next consideration. First let us construct the final state $\psi_{f,\beta}(r)$ for the electron photoemission into direction $\hat{k}_f$ from one center $\{n, \beta\}$ only. According to [9] it must be such function of continuum which has an asymptotic form of plane wave $\sim e^{i\mathbf{k}_f \mathbf{r}}$ and incoming radial waves at $|r - R_{n\beta}| \to \infty$. This final state is

$$\psi_f = \exp(ik_f R_{n\beta}) \sum_{lm} i^l e^{i\delta_{l\beta}} Y_{lm}(\hat{r}) Y^*_{lm}(\hat{k}_f) \varphi_l(r_\beta) \quad (8)$$

where $r_\beta = |r - R_{n\beta}|$. The scattering phase $\delta_{l\beta}$ for the orbital momentum $l$ is defined by the asymptotic of real radial function of continuum $\varphi_{l\beta}(r) \sim \frac{1}{r}\sin(kr - \pi l/2 + \delta_{l\beta})$. (According to the KKR approach one may consider that asymptotic form is achieved at the surface of the muffin-tin sphere.)

In similar manner the final state $\psi_f$ for the electron ejected from $N_s$ centers of the surface layer should be a function which at large $z > 0$ have an asymptotic form with common plane wave $\sim e^{i\mathbf{k}_f \mathbf{r}}$ and incoming spherical waves contributed from different centers.

If $k_f |R_{n\beta} - R_{n',\beta'}| > 1$ and if we neglect the secondary scattering processes, then inside each of nonoverlapping muffin-tin spheres surrounding center $(n\beta)$ of surface layer the final state wave function should just have a form (6) with complex coefficients $C_{L'\beta} \sim e^{i\delta_{l\beta}}$. Really the secondary processes synchronize the phases $\delta_{l\beta}$ of all contributions into the final state from different angular harmonics and different centers. The KKR bulk solution for the final state $\psi_f(k_f)$ found in [7] takes into account the phase and amplitude synchronization of all secondary processes, but it neglect the necessary additional synchronization and phase modulation coming from the boundary surface where solutions should be matched with the plane wave with momentum $k_f$ .

In order to study in qualitative manner the angular dependence of dichroism and its symmetry, it is sufficient to use the form (6) of the final state without specifying the values and phases of $C_{L'\beta}$ in (6). So we use Eqs.(5,6) for schematic representation of initial and final states to study the symmetry and possible angular dependence of dichroism manifested in ARPES. The components $F_\alpha$ of the matrix element (1) is expressed as a sum of integrals inside atomic spheres around centers $(\beta)$ for corresponding channels $l \to l'$

$$M_{R(L)} = A_\alpha(\zeta) F^\nu_\alpha(l'\hat{k}) \quad (9)$$

Here $A_\alpha$ are components of the vector potential (2) depending on the right or left polarization of CPL, $\zeta = \zeta_{R(L)} = \pm 1$, and $\hat{k} = \mathbf{k}_f/k_f$. Functions $F^\nu_\alpha(l', \hat{k})$ correspond to real initial orbitals $\nu = d_{x^2-y^2}, p_x, p_y$. To obtain them we use the selection rules $l' = l \pm 1$ for orbital angular momenta for integrals inside atomic spheres. For simplicity we retain only the matrix elements for the following transitions $p_{x(y)} \to s, d$ and $d_{x^2-y^2} \to p$ from the $O_{x(y)}$ and $Cu$ centers of $CuO_2$ plane. According the KKR calculations [7] such transitions give main contributions. Omitting of transition $d_{x^2-y^2} \to f$ at $Cu$ center does not change the symmetry properties of the calculated dichroism. This leads only to neglecting the small higher harmonics in angular dependence of the ARPES intensity.

The resulting expressions for functions $F^\nu_\alpha(l'\hat{k})$ are presented in Table. For the $p \to s, d$ transitions in oxygen they include also the factors

$$g_{x(y)} = s_{x(y)}/\sqrt{s_x^2 + s_y^2}; \quad s_{x(y)} = \pm \sin(k_{x(y)}/2); \quad (10)$$

They originate from angular dependence of real amplitudes $c_{x(y)}$ and $c_d$ of different orbitals in the initial band state (5) of Emery model (with effective parameters $\epsilon_d, \epsilon_p, t_{pd}, t_{pp}$). At $t_{pp} \ll t_{pd}$ the amplitudes in (5) are

$$c_{x(y)} = g_{x(y)} \sin\eta; \quad c_d = \cos\eta; \quad (11)$$

$$\tan 2\eta = 2t_{pd}(\cos k_x + \cos k_y)/(\epsilon_d - \epsilon_p).$$

Extension to large $t_{pp}$ does not change the symmetry of amplitudes.

The coefficients $C_{0(I,II)}(k)$ in table include: 1) a sum over the layers $\sum B_f^*(n_z)B_i(n_z)$ based on the phenomenological or tight-binding dependencies $B(n_z)$; 2) the phase factors $\exp(i\delta_{l'})$ coming from boundary conditions; 3) the reduced integrals $< l'\beta \parallel p \parallel l\beta >$ over angular variables after removing the $m$ dependence; 4) the radial integrals; 5) the factors $\sin\eta,\ \cos\eta$ from amplitudes (11).

Then the ARPES dichroism signal is

$$D(\varphi) = Im\{M(\Delta M)^*\}/(|M|^2 + |\Delta M|^2) \tag{12}$$

where $M = M_R + M_L$, $\Delta M = M_R - M_L$ and angles $\theta, \varphi$ describe a final momentum $\mathbf{k}_f$ . Dependence (12) may be presented as $D(\varphi) \sim \tilde{G}(k)\sin\varphi$ with even function $\tilde{G}(k)$ relative to reflection in mirror plane zx. According to (9) the quantities $M_{R(L)}$ are determined by complex constants $C_0, C_I, C_{II}$ whereas the rest angular functions listed in Table are real functions. It can be shown that the dichroism signal is zero if all coefficients $C_{L\beta}$ in (7) have the same phases $\delta_{\beta,l}$ or their differences are multiple to $\pi$. So a representation of final state with correct phases is significant for description of geometrical dichroism.

At $\hat{q}_\gamma = \mathbf{n}$ when photon impacts normally to the $CuO_2$ plane one obtains

$$\begin{aligned} M = \ & C_{II}\sin\theta\cos\varphi + g_x[C_0 - C_I(\cos^2\theta \\ & - \sin^2\theta\cos 2\varphi)] + g_y C_I \sin^2\theta\sin 2\varphi \end{aligned} \tag{13}$$

$$\begin{aligned} \Delta M = \ & -C_{II}\sin\theta\sin\varphi + g_y[C_0 - C_I(\cos^2\theta \\ & + \sin^2\theta\cos 2\varphi)] + g_x C_I \sin^2\theta\sin 2\varphi \end{aligned} \tag{14}$$

Here $\theta, \varphi$ are the polar angles of $\mathbf{k}_f$. It is seen from (11,12) that the dichroism signal $D(\varphi)$ is odd function $D(-\varphi) = -D(\varphi)$ and it go to zero at $\varphi = \pi$ or $\varphi = 0$. This is an expected property of geometrical dichroism.

Manifestations of geometrical dichroism depend on numerous parameters. Fig.2 illustrates an examples of functions $D(\varphi)$ for three angles $\theta_g = 0,\ \pi/6,\ \pi/3$ of the photon momentum in mirror plane $zx$ and for $k$ moving along boundary $|k_x \pm k_y| = \pi$ and $k_z = |k|$. We ascribe the following arbitrary values for relative amplitudes $|C_0/C_I| = |C_0/C_{II}| = 1.0$ and the relative phases $\{\delta_{l'=0}(O),\ \delta_{l'=2}(O),\ \delta_{l'=1}(Cu)\} = \{0,\ 3\pi/4, \pi/4\}$ of coefficients $C_0,\ C_I,\ C_{II}$ in different channels of oxygen and Cu centers. Two setup configurations with $x$ along $CuO$ bond or along diagonal direction are considered. Function $D(\varphi)$ is odd function of $\varphi$ and it vanishes at $\varphi = 0, \pi$. The calculated geometrical dichroism disappears for all $\varphi$ if all phase differences $\delta_l - \delta_{l'} = \pi m$ are multiple to $\pi$. This is just the case for the Cu- and O- contributions to the matrix element calculated in [7]. There the standard KKR bulk wave functions were used and an additional phase modulation were neglected. At a normal photon impact ($\theta_\gamma = 0$) a dichroism signal is zero on each mirror plane of tetragonal lattice, i.e. at $\varphi = \frac{\pi}{4}m$.

Now we take into account the spin-orbit interaction on Cu with a constant $\lambda$

$$V_{LS} = \lambda \sum_n \mathbf{L}_n \mathbf{S}_n \tag{15}$$

Then the initial band function $\psi^i_{k\sigma}$ transforms to $\psi^i_{k\sigma} + \delta\psi$ in a way equivalent to replacement of $d^\dagger_{x^2-y^2,\sigma}$ in (5) by

$$d^\dagger_{x^2-y^2,\sigma} + C_\lambda[2i\xi_\sigma d^\dagger_{xy,\sigma} - \xi_\sigma d^\dagger_{zx,-\sigma} - i d^\dagger_{zy,-\sigma}] \tag{16}$$

in Eq.(5,4). Here $\xi_\sigma = \sigma/|\sigma| = \pm 1$ and $C_l \sim \lambda/2\delta E$ where $\delta E$ is the energy difference of the d-orbitals of $x^2 - y^2$ and $xy, yz, xz$ symmetries. Additional contribution to $\psi^i_{k\sigma}$ leads to changes $M \to M + \delta M$, $\Delta M \to \Delta M + \delta\Delta M(\sigma)$ in Eqs.(10, 11,12). The TRSB dichroism signal at the normal photon impact ($\theta_\gamma = 0$) is determined then by a quantity

$$\delta\Delta M = \xi_\sigma 4 C_\lambda C_{II} \sin\theta\cos\varphi \tag{17}$$

As a result the dichroism signal $D(\varphi, \sigma)$ of photoemission with the final momentum $k_f$ and spin projection $\sigma$ of the ejected electron has a form

$$D(\sigma, k) = A\sin\varphi - \frac{\xi_\sigma Re(MC^*_{II})}{|M|^2 + |\Delta M|^2} 4C_\lambda \sin\theta\cos\varphi \tag{18}$$

Here $M, \Delta M$ and $C_{II}$ are determined by Eqs.(13,14,7) and by functions from Table. Only linear in $\lambda$ term is retained in (16). It is determined only by admixture of $d_{xy}$ orbital in Eq.(18). The contributions from d-orbitals of $xz,\ yz$ symmetries in (16) are of a 2-nd order of magnitude in $\lambda$. The second term in (18) is even function of $\varphi$

and have nonzero value at $\varphi = 0$ or $\pi$ when all three vectors $\mathbf{q}_\gamma, \mathbf{n}, \mathbf{k}_f$ lye in the mirror plane xz and geometrical dichroism disappears.

Since a sign of $D(\varphi = 0)$ depends on sign of spin projection $\sigma$ of ejected electron, the overall dichroism $D = \sum_\sigma D(\sigma, \varphi)$ should be zero for initial paramagnet (PM) state of system. So, for PM state the dichroism at $\varphi = 0$ or $\pi$ would be observed only if one selects the ejected electrons with definite spin projection on $\mathbf{n}$. For this PM state the time reversal symmetry is broken just by a measurement of spin polarization of photoelectron.

However, there are the TRSB states in which the different regions of $k$ space are characterized by different spin polarization. For example, for the ground state with a spiral spin structure the TRSB effect manifests in ARPES by the nonzero overall dichroism at arrangement of all vectors $\mathbf{q}_\gamma, \mathbf{n}, \mathbf{k}_f$ in the mirror plane.

Let us demonstrate the polarization selectivity of the level occupancies in $k$-space for the spiral state of the 2D $t - t' - U$ Hubbard model. Calculations were carried out for model with $U/t = 6$, $t'/t = 0.1$ at doping 0.15 holes per site. The spiral mean-field (MF) solution is characterized by average spins $< \mathbf{S}_n >= d(\mathbf{e}_x \cos Qn + \mathbf{e}_y \sin Qn)$ rotating in the $xy$ plane. We study the MF states of two types - with the spirality vectors

$$Q_I = (\pi - \delta Q_x, \pi), \quad Q_{II} = (\pi - \delta Q, \pi - \delta Q) \qquad (19)$$

along $CuO$ bond or along diagonal direction. The spectral function $A_\sigma(k, \omega)$ at $\omega = 0$ for definite spin projection $\sigma$ on $z$- axis (perpendicular to the spin rotation plane) is equal to

$$A_\sigma(k, \gamma) = \sum_{if} | < \psi_f | c_{k\sigma} | \psi_i > |^2 f(E_i) \delta_\gamma(E_i - E_f) \quad (20)$$

Here the Fermi function $f(E_i)$ depends on the one-electron levels of MF solution and $\delta_\gamma(x)$ is the $\delta$-function broadened with parameter $\gamma \sim 0.05t$. Fig.3 presents an image of the spin-selective and overall spectral functions $A_{\sigma=\uparrow}(\mathbf{k})$ and $A(\mathbf{k}) = \sum_\sigma A_\sigma$ at $\omega = 0$ for two types of spiral states. Dark and light gray lines in Fig.3 correspond to main and shadow spin-selective ($\sigma =\uparrow$) sections of Fermi surfaces. Similar images for $\sigma =\downarrow$ are obtained from those for $\sigma =\uparrow$ by inversion $\mathbf{k} \to -\mathbf{k}$. The spin dependence of the level occupancy in $k$ space is connected with the spin currents $J_\uparrow = J_\downarrow \sim Q$ existing in spiral state.

Thus, the TRSB state with spiral spin structure certainly has a spin-selective sections of Fermi surface. As a consequence, one can observe the TRSB dichroism of the ARPES signal even at coplanar arrangement of the setup vectors $\mathbf{q}_\gamma, \mathbf{n}, \mathbf{k}_f$ in mirror plane. Two factors are decisive here: 1) The ARPES signal corresponds to a definite local region of $k$ which for given spirality vector $Q$ is associated with definite spin polarization; 2) According to Eq.(16,17) a definite spin polarization induces via the spin-orbit interaction the orbital angular momenta on Cu centers and corresponding nonzero dichroism at coplanar setup configuration.

In order to estimate effect we use the spin-orbit constant $\lambda \sim 800$ $\mathtt{cm}^{-1}$ following from excitation spectrum of $Cu^I, Cu^{II}$ [10] and a splitting of d-orbitals $\delta E = E_{x^2-y^2} - E_{xy} \sim 1 \div 2$ eV in crystal field. Then one has a value $C_\lambda = 0.0025 \div 0.005$ for amplitude in (16). At setup configuration $\theta_\gamma = 0$, $\theta = \theta_k = \pi/4$, $\varphi = \pi$ or 0 and at the same arbitrary chosen coefficients (7) as were used in Fig.2 ($|C_I/C_0| = |C_{II}/C_0| = 1$, $\delta_{\beta,l} = 0, 3\pi/4, \pi/4$), one obtains for the TRSB dichroism $max|D| = 0.033 \div 0.066$ at $k$ corresponding $\varphi = 0$ $\mathtt{or}$ $\pi$ and lying in mirror plane. This value is consistent the TRSB dichroism signal $\sim 3 \div 5\%$ observed in UD cuprates [3].

In conclusion, it is shown here that the TRSB dichroism observed in the ARPES spectra of the UD cuprates may be connected with a local spiral spin order in system. This hypothesis differs from the model TRSB state proposed by Varma et al. [4,5] who connect the TRSB with aligned charge circular microcurrents on plaquettes of $CuO_2$ plane. Instead, the spiral spin order means appearance of the local spin currents $\mathbf{J}_\uparrow = -\mathbf{J}_\downarrow$ of the macro-scale, about the domain size. Existence of different domains with different signs and values of the TRSB dichroism signal has been shown by study a set of samples of UD BSCCO in [3]. The following test for new hypothesis may be proposed. The rotation of sample on 180° around z-axis does change a sign of the TRSB dichroism $D(\varphi = \pi)$ in our hypothesis and does not change the sign in case of the TRSB state constructed in [4]. In the former case the rotation changes the signs of the

spin currents and of spin polarization. Relative signs of the TRSB dichroism signal at different mirror planes of cuprate for two types of spiral states (19) and for the state proposed by Varma are illustrated in Fig.4. These signs may be measured only if the ARPES signal comes from the same domain of a sample before and after its rotation and if the spin currents of spiral state are pined during rotation of sample. Note, that in case of the ferromagnet alighnment of spins in the surface layers, the TRSB dichroism would have the same signs at all directions in mirror planes of the lattice.

A great sensitivity of the Fermi surface (FS) to the spin structure puts the questions important for understanding the pseudogap state of BSCCO: Whether the observed FS is a composed result coming from several domains with different currents? What is a dynamics of these currents and domains in the UD cuprates? May the spin fluctuations be frosen near the surface into a static domains with spiral or ferromagnet spin order? Additional test for the supposed local spiral order is possible. One can measure the spin polarization $< \mathbf{S} >$ of electrons ejected from different sections of the Fermi surface and to check the correlations of direction of $< \mathbf{S} >$ with the sign of the TRSB dichroism signal $D(\varphi)$ at $\varphi = \pi$. Such a program requires a spin-selective detection of photoelectrons.

Work is supported by Russian Fund of Fundamental Research (Projects No. 00-03-32981 and No. 00-15-97334). Author is grateful to A.A.Ovchinnikov and V.Ya.Krivnov for useful discussions.

[1] T.Timusk, B.Statt, Rep.Progr.Phys. **62**, 61 (1999)

[2] J.C.Campusano, M.R.Norman, M.Raderia, in Physics of Conventional and Unconventional Superconductors. ed.K.H.Benneman, J.B.Ketterson, 2002; cond-mat/0209476.

[3] A.Kaminsky, S.Rosenkranz, H.M.Fretwell, J.C.Campuzano, Z.Li, H.Raffy, W.G.Cullen, H.You, C.G.Olson, C.M.Varma and H.Höchst, E-print Archive, cond-mat/0203133.

[4] C.M.Varma, Phys.Rev.B**61**, R3804 (2000).

[5] M.E.Simon and C.M.Varma, E-print Archive, cond-mat/0201036.

[6] Y.Sakisaka, J.Electr.Spectr.Relat.Phen.**66**, 387 (1994)

[7] M.Lindroos, S.Sahrakorpi and A.Bansil, E-print Archive cond-mat/0109039, Phys.Rev.B**65**, 054514 (2002).

[8] A.Damascelli, Z.X.Shen and Z.Hussain, E-print Archive, cond-mat/0208504, to be publish in Rev.Mod.Phys.

[9] L.Landau and L.Lifshitz, Quantum Mechanics. M.Nauka, 1989.

[10] Atomic Energy Levels, ed. R.F.Bacher, S.Goudsmoth, McGraw-Hill Book Company, N.Y.-London, 1932.

TABLE I. Functions $F^{\gamma}_{\alpha}(l', \hat{k})$ determining the $\alpha$-components of matrix element in Eq.(1). Index $\gamma$ numerates the contributions originated from different orbitals of initial state: from $p_{x(y)}$ orbitals of oxygens $O_{x(y)}$ or $d_{x^2-y^2}, d_{xy}$ orbitals of $Cu$; final channels $s, p, d$ correspond to angular momenta $l' = 0, 1, 2$. Functions $G_{x(y)}$, $L_k$, $g_x$ and $g_y$, $P_k$ are even and odd functions relative to mirror planes zx correspondingly.

| $\psi_{i\beta}$ | $\psi_f$ | $F_x$ | $F_y$ | $F_z$ |
|---|---|---|---|---|
| $p_x$ | $s$ | $C_0 g_x$ | 0 | 0 |
| $p_x$ | $d$ | $C_I g_x G_x$ | $C_I g_x P_k$ | $C_I g_x L_k$ |
| $p_y$ | $s$ | 0 | $C_0 g_y$ | 0 |
| $p_y$ | $d$ | $C_I g_y P_k$ | $C_I g_y G_y$ | $C_I g_y L_k$ |
| $d_{x^2-y^2}$ | $p$ | $C_{II} \sin\theta \cos\varphi$ | $-C_{II} \sin\theta \sin\varphi$ | 0 |
| $d_{xy}$ | $p$ | $C_{II} \sin\theta \sin\varphi$ | $C_{II} \sin\theta \cos\varphi$ | 0 |

[a] $G_{x(y)} = \pm \sin^2\theta \cos 2\varphi - \cos^2\theta + 1/3$

[b] $g_{x(y)}$ are determined by Eqs.(10)

[c] $L_k = \sin 2\theta \cos\varphi$; $\quad P_k = \sin^2\theta \sin 2\varphi$

FIG. 1. The setup configuration of the ARPES experiment [3]. The propagation vector $\mathbf{q}_\gamma$ of CPL lies in a mirror plane xz and $\mathbf{k}_f$, $\mathbf{k}$ are the final momentum of ejected electron and its component in $CuO_2$ plane (xy plane).

FIG. 2. Dependence of geometrical dichroism $D(\varphi)$ on the azimuthal angle $\varphi$ of vector $\mathbf{k}_f$ for k moving along the nesting lines $|k_x \pm k_y| = \pi$. Solid, dashed and thin curves correspond to angles $\theta_\gamma = 0,\ \pi/6,\ \pi/3$ of the photon momentum $q$. Setup configurations with x along diagonal direction or along the $CuO$ bonds refer to left or right graphics. Arbitrary taken coefficients (7) are given in text.

FIG. 3. The images of the spin-selective (plots a,c) and overall (plots b,d) spectral functions $A_\uparrow(k,\omega),\ A(k,\omega)$ at $\omega = 0$ in Brillouin zone. Main and shadow Fermi surface are shown for the spiral states with the spirality vectors $Q = Q_I$ or $Q = Q_{II}$ from (19) (plots a,b or c,d correspondingly) .

FIG. 4. Relative signs of the TRSB dichroism signal for $\mathbf{k}$ lying on different mirror planes of lattice for spiral states with spirality vectors $Q_I$, $Q_{II}$ from (19), or for state proposed by Varma (VS).

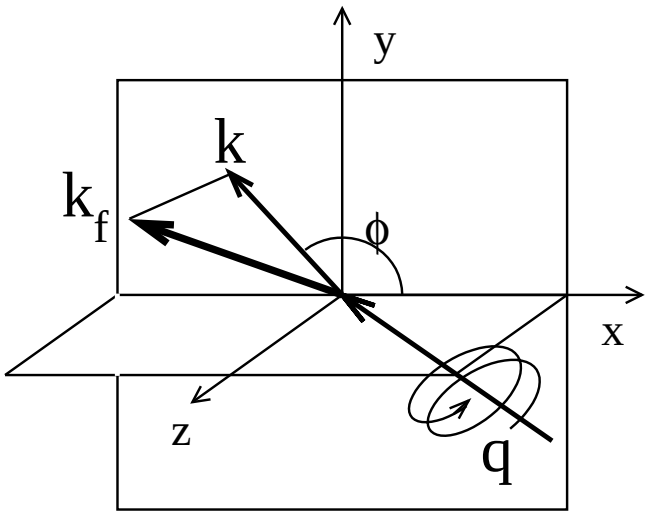
y
k
$k_f$
ϕ
x
z
q

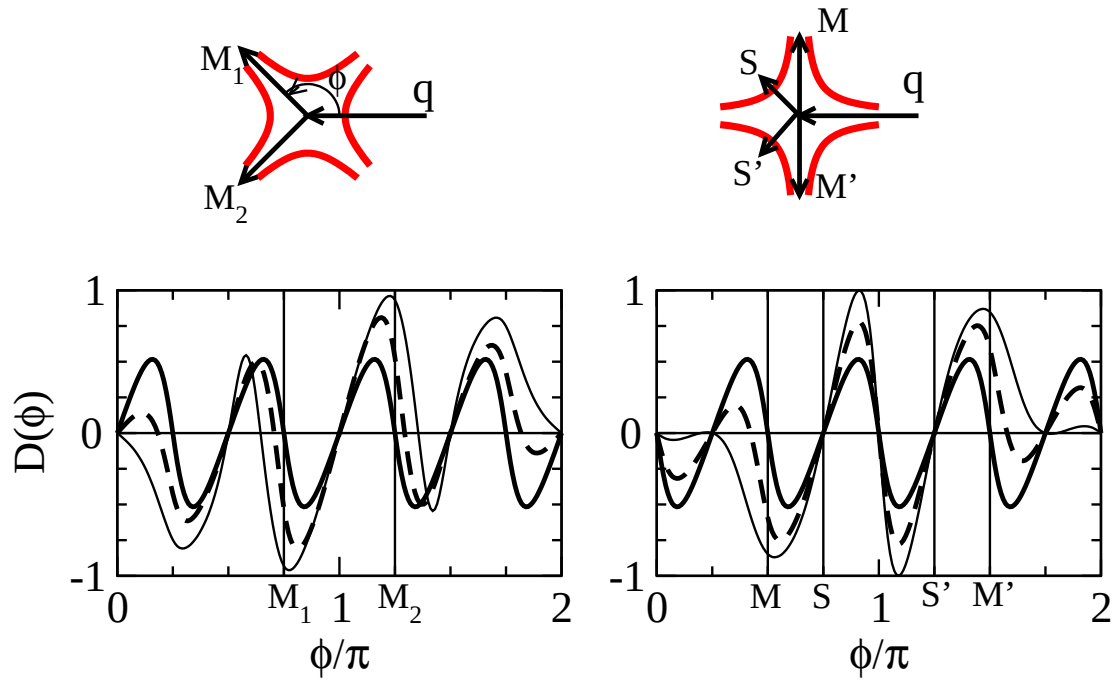
M1
ϕ
q
M2
M
S
q
S'
M'
1
0
-1
D(ϕ)
M1
1
M2
2
ϕ/π
1
0
-1
0
M
S
1
S'
M'
2
ϕ/π

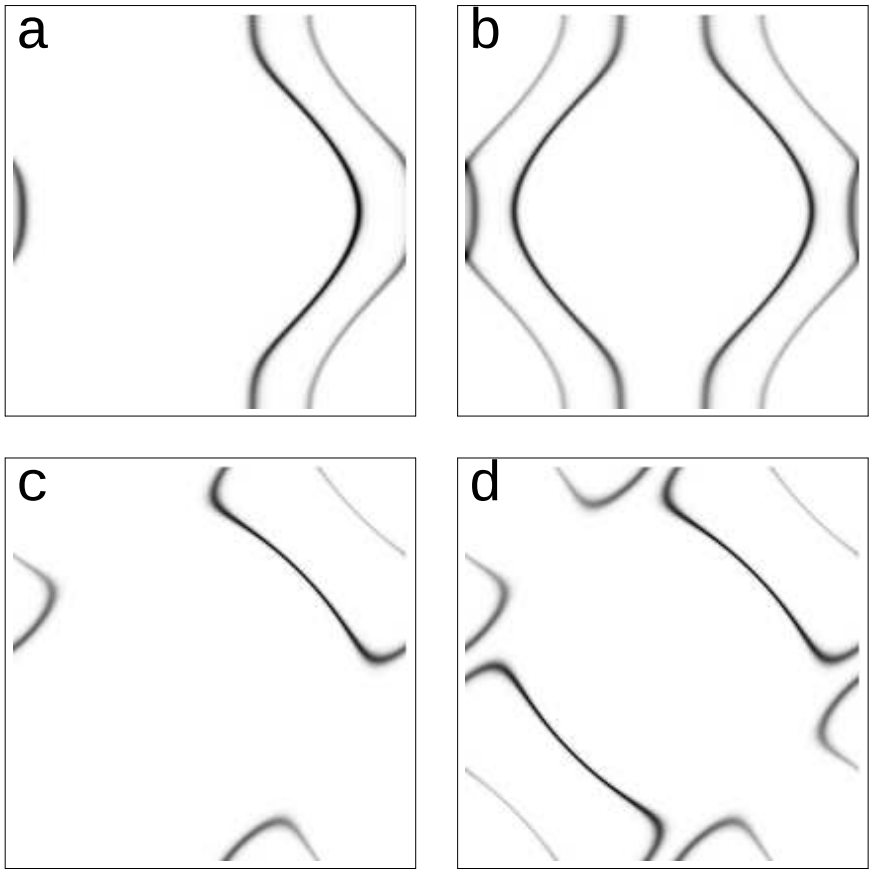
a
b
c
d

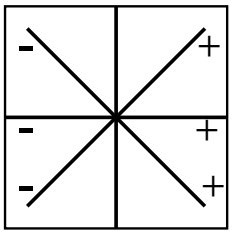


$Q_I$

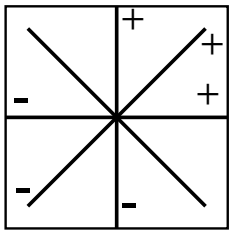


$Q_{II}$

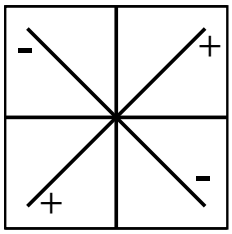


VS